CAVITY DETECTION IN URBAN ZONES OF MEXICO CITY.

René E. Chávez*, Andres Tejero, and Javier Urbieta

Instituto de Geofísica, and Fac. de Ingeniería, UNAM

ABSTRACT

Cavities and shallow fractures on mined regions beneath urban sites of Mexico City are a high-risk problem. Electric tomography has been applied to successively detect and map these types of structures to the western side of the city. The method developed by Loke and Barker was employed to image the electrical distribution at depth. GPR (Ground Penetrating Radar) was also used to confirm the results obtained. The area selected contains a high rate of population and found in the hilly portion of the city, within the Mexican Valley. Results are very encouraging, demonstrating that a multicomponent geophysical survey help to locate and characterize areas of high risk.

INTRODUCTION

Mexico City constitutes one of the largest concentrations of human activities in the world, with a population of about 20 million people. It is located in the Trans-Mexican Volcanic Belt (TMVB), in the central Mexico.

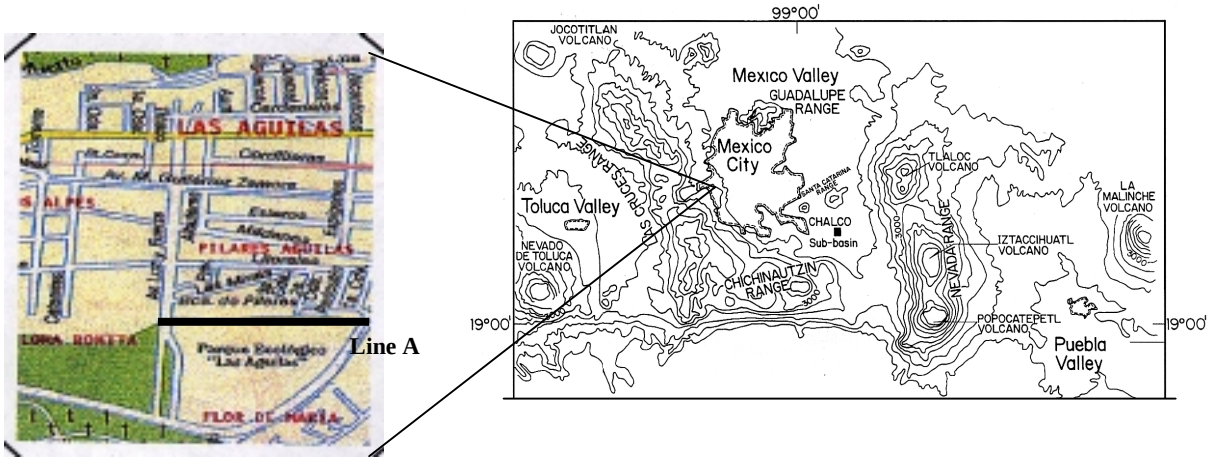

Fig.1 Location of the area under study (left) within Mexico City urban zone (right).

The TMVB is a Plio-Quaternary calc-alkaline province that crosses Mexico form west to east. The region comprises most of the historic and present-day volcanism of Mexico and includes andesitic-dasitic stratovolcanos, cinder cone fields, isolated occurrences of rhyolitic volcanism, and major rhyolitic centers. Mexico City is located in a basin at a height of 2200 m a.s.l. and about 300 km east of the Central America Trench. Volcanic ranges (Sierras) confine the basin: the Sierra Nevada on the east, the Sierra de Chichinautzin on the south, the Sierra de las Cruces on the west, and the Sierra de Guadalupe on the north (Fig.1). It is interesting to point out that Sierra Nevada includes the Popocatepetl an andesitic-dasitic stratovolcano volcano, in activity nowadays.

The confined nature of this intramontane valley directly affects air quality, water supply and urban development. The different anthropogenic processes defining the urban an industrial development also influence the population's quality of life. Therefore, administering services for the inhabitants of this city is a big challenge (Campos et al., 1997).

On top of these problems, comes the insufficient housing and sheltering for the population, a problem that has increased during the past 35 years. During the end of the forties and the fifties, and because of the anarchical growth of the urban areas, most of the material used for constructing purposes was obtained from mines excavated in the western Sierras. Such materials were employed to build houses, apartment and governmental buildings in downtown Mexico. When this industry came to an end at the beginning of the sixties, most of these mines, turned in cavities were abandoned or refilled with debris. Because of its size, caves were later used as shelters for entire families, or had other uses by the people in the neighborhood. Nowadays, location of these structures is unknown. Low-, middle- and high middle neighborhoods have settled on top of mined zones for the past 20 years. Many accidents have occurred ever since,

caves have collapsed and complete homes have been literally swallowed by the ground.
The University of Mexico and the Alvaro Obregon County (one of Mexico's capital municipalities) launched in 1995 a joint research program to carry out geophysical work to define the location of hazard zones. This study presents the results in an area (Fig.1, left) that included resitivity and GPR measurements. Results are encouraging, and resistivity imaging methods shown a helpful tool to define these structures.

GEOLOGICAL SETTING

Mexico City was founded originally on a small island in a lake confined by volcanic ranges. It is located in the central portion of the TMVB (Pasquare et al., 1987). The area under study is found to the southwestern portion of the Valley of Mexico (Fig.1). The relief is abrupt and composed of a series of step hills and deep gorges. Surface rocks are deposits of igneous materials thrown by volcanoes within the Sierra de Las Cruces. These geological events produced avalanches of pyroclastics, tuffs and breccias deposited in the lowlands of the Sierras. The volcanic rocks conforming the relief in the area of study are of Cenozoic age, and known as the Tarango formation. This geological horizon is a sequence composed of slabs of sands, grabbles pumices interbedded with clays and sandstones. Pumice was the product of violent volcanic explosions, fragments were dragged by the wind to very big distances from the crater and evenly deposited in the lower zones. The stratigraphic column of the Tarango formation is divided in two units. Unit A is the youngest and it is found at the gorge slopes and consists of fragmented rocks dragged by water flows. These landslides were produced by rainy water saturation, moving down at big speeds by gravity effects. These types of rocks are well compacted housed in a sand matrix with sharp corners. Unit B is a pyroclastic sequence, a product of volcanic eruptions. Pumice, travertine, sand and alluvial material are the rocks forming this unit. Such rocks were employed to make light bricks. This unit forms the 'crown' or tops of the hills in this area. Most of the mining industry exploited the lower sections in the pumitic sands. Main mines are located here and stratigraphic position defines quality and hardness of materials. Cavities found in this unit are at depths ranging from 5 to 8 m. Size of main chambers is variable, from 2 to 3 m up to 30 m.

ELECTRICAL TOMOGRAPHY

Observations are normally made using a computer controlled system with a large number (25 or more) of electrodes laid out in a profile at constant interval. The data are displayed in a false color image depicting lateral and vertical variation of resistivity in the subsurface. However, it depends on the subsurface resistivity distribution, and on the electrode geometry.
Electrical imaging can be divided into two steps: (1) concerning the collecting data process and (2) with the inversion approach to estimate the true subsurface resistivity. Mathematical modelling can be accounted in several steps: (1) apparent resistivity is computed employing a finite difference or finite element method, (2) select the non-linear optimization technique, (3) evaluate the elements of the Jacobian matrix, and (4) solve the system of equation.
Data was collected by using a dipole-dipole array with 3 m electrode spacing and up to 16 levels of determination. The method developed by Loke and Barker (1995,1996) was employed.
The j-observed data is calculated by using a first-order Taylor approximation, as:

$$e_j^{est} = F_j(P_{est}) + \sum_{k=1}^{M} \frac{\partial F_j(P_{est})}{\partial p_k} \delta p_k \qquad \textbf{(1)}$$

where j=1,2,3.....N. $\mathbf{P}_{est}$ is the estimated parameters vector of the model and if we defined the difference as:

$$\delta e_j = e_j^{obs} - e_j^{est}(P_{est}),$$

for each observed data we get :

$$\mathbf{g} = \mathbf{J}\,\delta\,\mathbf{P} \qquad \textbf{(2)}$$

where **J** is the Jacobian matrix with elements:

$$J_{jk} = \partial F_j / \partial p_k ,$$

and $\delta\mathbf{P}$ is the perturbation vector and **g** is the vector of differences. Following Loke and Baker (1995), the equation (2) can be solved for $\delta\mathbf{P}$ as:

$$\delta\,\mathbf{P} = (\mathbf{J}^T\mathbf{J} + \lambda\,\mathbf{C}^T\mathbf{C})^{-1}\mathbf{J}^T\mathbf{g} \qquad . \qquad \textbf{(3)}$$

Sixth International Congress of the Brazilian Geophysical Society

Here λ is a damping factor and **C is** a flatness filter which is used to constrain the smoothness of the perturbations to the model parameters to some constant value (Sasaki, 1992). The upper symbol **T** indicates the transport matrix. A method named *least square deconvolution* (Loke and Baker, 1995) is used to estimate the jth element of the jacobian matrix. Loke and Baker update the matrix applying the Broyden's method. Then, it is not necessary to calculate the entire Jacobean matrix for each iteration, the process is more stable and the convergence rate is fast and used to solve for many non-linear problems (Broyden, et al, 1972).

RESULTS

A cave in line A is well known and is used as a testing site. Electrical imaging and GPR methods are employed here. This is set on top of the known feature, few meters away from a gorge. Depth to the top is approximately 4 m. Fig.2 displays the results of the electric survey. Top of figure shows the observed apparent resistivity, bottom displays the computed values. Fit between both diagrams is not reached as satisfactorily as one would like. Since the surveyed profile was located close to the gorge edge, the two-dimensional condition does not fully hold. However, the electrical image shows the cavern at the center of the diagram (x=29 m), at a depth of about 4.4 m, with resistivities ≤205 ohm.m. Another cavern having similar values can be observed to the left at x=12 m and at a depth of 2.4 m. This is shallower and smaller (about 3 m in diameter).

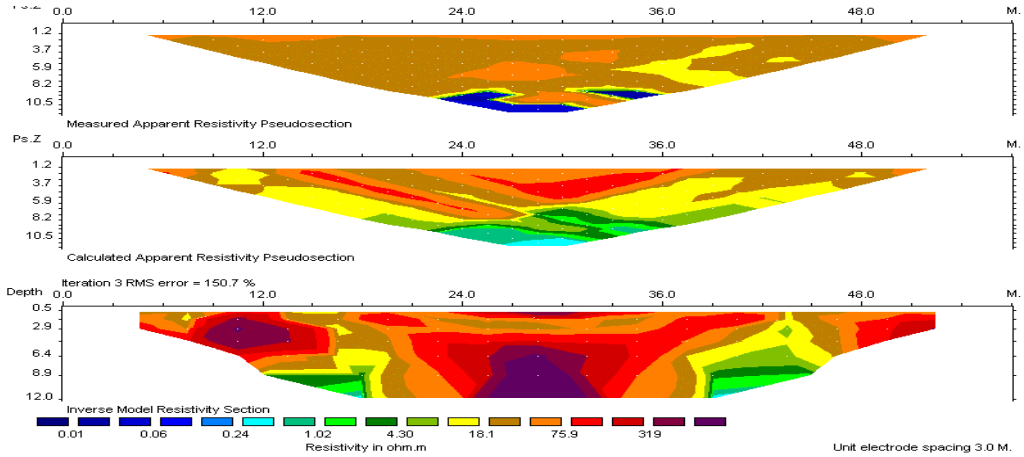

Fig.2 Resistivity image on line A.. Cavity location is seen at the center of imaged section (Bottom)

In order to study the resolution of electrical tomography a (GPR) profile was carried out over the electrical profile A, nevertheless the length of line was smaller (Fig.3). The GPR used was an EKKO IV of Sensor & Software. A 2 meters antennas separation, with a nominal frequency of 100 Mhz. and a step size of 0.5 meters was employed. The inferred velocity of electromagnetic waves in this type of terrain was estimated to be 0.125 m/ns. Fig.3 shows the hyperbolic classic signal for a top of a cave. It can be observed at x=24 m, to a depth of 4 m.

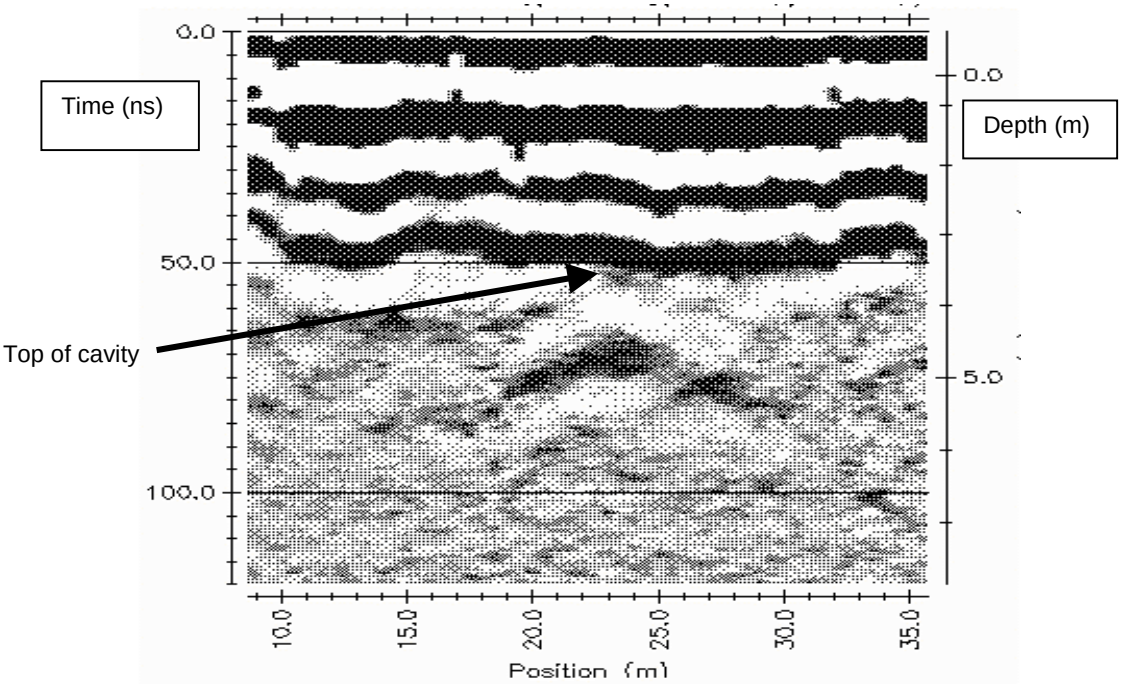

Sexto Congresso Internacional da Sociedade Brasileira De Geofísica

Fig.3 GPR line along resistivity profile A. Cave is located at x=24 m at a depth to the top of 4 m.

These parameters correlate well with the electrical tomography done on the same GPR profile, on comparison with Fig. 2.

CONCLUSIONS

Electrical imaging produces satisfactory results, when geological structures can be approximated to 2D models. It is important to point out that this approach can resolve complex structures, which can be masked by noisy resistivities. Such effect occurs when analyzing the apparent resistivity maps. The interpretation process applied to the resistivity sections shown is stable and in few iterations is possible to arrive to a satisfactory solution. Computer time takes few minutes to obtain reasonable models. The dipole-dipole method used in this study is very efficient and suitable for this type of methods.

REFERENCES

Broyden, C. G., 1972. Quasi-Newton method: in Murray, W., Ed., Numerical Methods for Unconstrained Optimization, Academi Press, Inc., 87-106.

Campos, J. O., Delgado-Rodríguez, O., Chavez-Segura, R. E., Gómez-Contreras, P., Flores-Márquez, E. L., and Birch, F. S., 1997. Thesubsurface structure of the Chalco sub-basin (México City) inferred from geophysical data: Geophysics, ***62****, 23-35*

Loke, M. H. And Barker, R. D., 1996. Rapid least-squares inversion of apparent resistivity pseudosection by quasi-newton method: Geophys. Prosp., ***44****, 131-152.*

Loke, M. H. And Barker, R. D., 1995. Least squares deconvolution of apparent resistivity pseudosections: Geophysics, ***60****, 1682-1690.*

Pasquare, G., Vezzoli, L., and Zanchi, A., 1987. Morphological and structural model of Mexican Volcanic Belt: Geofisica Internacional, ***26,*** *159-176.*